Precoding for Non-coherent detection of continuous phase modulations

Charles-Ugo Piat-Durozoi[†‡], Charly Poulliat[‡], Nathalie Thomas[‡], Marie-Laure Boucheret[‡], Guy Lesthievent[*], Emmanuel Bouisson[*], [†]TéSA, [‡]University of Toulouse, INPT/IRIT and [*]CNES Toulouse, France
Email: charles-ugo.piat@tesa.prd.fr, {vorname.name}@enseeiht.fr, {vorname.name}@cnes.fr

***Abstract*—Non-coherent trellis based receiver (TBR) is an effective method to demodulate noncoherent continuous-phase modulated sequences. However it requires to increase the observation length to reach the performance of classical coherent TBRs. Furthermore it appears that both receivers offers different behaviours when considered in a bit-interleaved coded modulation (BICM) system using iterative decoding. Indeed, trellis based outer coding schemes performing well in coherent regime generate error floors in non-coherent regime. In this paper, we show that precoding of the continuous phase modulation (CPM) encoder can deal with the latter issue. The optimization of this non-coherent precoding relies on different objectives than the existing precoding methods introduced in the coherent case. The optimization relies on some asymptotic arguments enabling an efficient BICM scheme using iterative decoding. Using the proposed precoding approach enables to remove error floors in the non-coherent regime while enabling transparent use in the coherent case.**

***Index Terms*—Non-coherent, precoding, continuous phase modulation, extrinsic information, information rate.**

I. Introduction

CPM is a particular modulation having a constant envelop waveform leading to excellent power efficiency [1], [2]. A second important aspect of CPM is the phase continuity yielding better spectral occupancy. The phase of a CPM signal for a given symbol depends on the cumulative phase of previous transmitted symbols known as the phase memory. Hence the decision taken on the current symbol must take into account the previous ones. Two types of CPM can be distinguished, partial response CPM which has a memory strictly greater than one symbol and full response CPM whose memory is exactly equal to one. Another important element of CPM is the modulation index which could restrain, in a particular case, the set of the phase memory to a finite set. A well-known full response CPM is the continuous phase frequency shift keying (CPFSK) described by a rectangular phase response. This modulation suits well to low rate data transmission applications such as telemetry launchers (Ariane, Vega, Soyuz...). Partial response CPMs are also used in several communication systems. For instance, Gaussian minimum shift keying (GMSK) with 3 symbols in memory and a gaussian pulse bandwidth of 0.3 is the modulation specified for GSM standard. Other type of applications concern aeronautical/satellite or military/tactical communications.

Transmission channels undergoing unknown phase shift are called non-coherent (by opposition to coherent channel). Detection methods for CPM adapted to both channels were studied in [5], [10], [13]. It appears that their associated receiver offers different behaviour regarding asymptotic performance illustrated by extrinsic information transfer (EXIT) charts [15]. EXIT chart is a tool used to study the exchange of extrinsic information between the soft input and the soft output of decoders. More broadly, it is used to analyze the convergence behaviour of codes and to derive in certain cases an approximation of the achievable rate [17]. For the coherent case, it can be shown that EXIT curves of most widely spreaded CPM in use have EXIT charts reaching the point $(1, 1)$, except if some particular precoding is used. When BICM CPM schemes are considered, this convergence enables the use of efficient turbo-detection schemes involving simple outer coding schemes based on convolutional codes such as in the DVB-RCS2 standard [8] or based on sparse graph based codes [11], [12]. For the non-coherent case, it has been pointed out by [9] that non-coherent EXIT curves do not converge to point $(1, 1)$ contrary to the coherent case. As a result, non-coherent iterative detection associated with a classical convolutional code or sparse graph based codes that have been optimized for the coherent case would tend to have error floors and/or capacity penalty. To deal with this issue, one solution would be to design some precoding schemes that would enable the use of classical schemes. This is the purpose of this paper.

Some previous works on precoding were carried out on CPM in coherent regime. [6], [7] proposed a precoding to maximize the so-called *pragmatic capacity* (ie. the information rate reached without iterating) and to ensure to operate close to the capacity. In the general case, symbols are modulated through a continuous phase encoder (CPE) following Rimoldi's representation [3] which enables in particular to get a time-invariant trellis structure of CPM modulations. This decomposition induces a natural mapping between information symbols and CPM waveforms, yet [6] has shown that it may be possible to improve the pragmatic capacity by changing this mapping. The approach consists in modifying the CPE structure by adding a state-dependent input mapping. The new mapping is called in [6] *dynamic mapping* and can be seen as a rate one precoding. The precoding input symbols are obtained by combining the information input symbols, the precoding symbols in the CPM memory and the accumulated precoding symbols taken from the start of the message. As a result, the obtained scheme serially concatenated with a convolutional code performs close to the capacity without iterating which can be also illustrated by almost flat EXIT curves in the binary case. This enables the use of efficient

outer coding schemes without the need for iterative detection. Thus the precoding is able to change EXIT trajectories while keeping ***the same information rate***: this asset will be used in the sequel. However the method is efficient only for binary CPM, indeed a significant gap appeared between the M-ary pragmatic capacity and the M-ary maximal information rate. Furthermore, it is not suited to the non-coherent case since it is necessary to know perfectly the accumulated phase to demodulate. In this paper we proposed a different (dual) approach for a precoding scheme adapted to the non-coherent regime enabling efficient iterative detection while ensuring backward compatibility with the coherent case.

The remainder of this paper is organized as follows. The section II provides a detailed exposition of the system model and the structure of the non-coherent receiver. The precoding and optimization procedure are presented in Section III. Section IV gives some simulation results while Section V concludes the paper.

II. System Model

At the emitter, a binary message vector $\mathbf{b}=[b_0,\cdots,b_{K_b-1}]\in\mathbb{F}_2^{K_b}$ is encoded into a binary codeword $\mathbf{c}=[c_0,\cdots,c_{N_b-1}]\in\mathbb{F}_2^{N_b}$ using an error correcting code of rate $R=K_b/N_b$. $\mathbf{c}$ is then interleaved and mapped into a sequence of N_s M-ary symbols from the considered modulation. Let $u_0^{N_s-1}=\{u_0,...,u_{N_s-1}\}$ be the set of N_s symbols belonging to the M-ary alphabet $\{0,...,M-1\}$. We note $m=log_2(M)$ (with M being a power of 2). The obtained symbols are then modulated following the CPM modulation rule using Rimoldi's representation (see [3]). This can be seen as the serial concatenation of a continuous phase encoder (CPE) and a memoryless modulator. First, the CPE ensures the continuity between the transmitted continuous-time waveforms by accumulating the phase of each modulated symbol.

$$\phi_{k+1}=\phi_k+2\pi h u_{k-L+1} \tag{1}$$

h is the modulation index ($h=P/Q$, with P and Q relatively prime) and ϕ_k is the accumulated phase at the start of the k^{th} symbol. We note $\mathcal{Q}$ the set of Q values taken by the ϕ_k. L is a strictly positive integer referred to as the memory of the CPM. Then, the memoryless modulator maps the output of the CPE into a set X of M^L continuous-time waveforms. At the k^{th} symbol interval, the subset $u_{k-L+1}^k=\{u_{k-L+1},...,u_k\}$ matches $x_i(\tau)$ corresponding to the i^{th} signal of $X=\{x_i(\tau), i=0...M^L-1\}$ with [3], [4]

$$x_i(\tau)=\frac{A(\tau)}{\sqrt{T}}\cdot e^{j4\pi h\sum_{n=0}^{L-1}u_{k-n}q(\tau+nT)},\tau\in[0,T), \tag{2}$$

where $A(\tau)$ represents the Rimoldi representation's data independent terms and the index i is determined as follows

$$i=\sum_{n=0}^{L-1}u_{k-n}\cdot M^{L-1-n} \tag{3}$$

and

$$A(\tau)=e^{j\pi h(M-1)\left(\frac{\tau}{T}+(L-1)-2\sum_{n=0}^{L-1}q(\tau+nT)\right)}. \tag{4}$$

In the expression above, T is the symbol period and the function $q(t)$ is the phase response satisfying $q(t)=0$ if $t\leq 0$, $q(t)=\frac{1}{2}$ if $t>LT$ and $q(t)=\int_0^t g(u)du$ if $0<t\leq LT$. $g(u)$ represents the CPM frequency pulse. Finally, the complex baseband representation of the transmitted continuous-time CPM waveform $\forall\, t\in[kT;(k+1)T)$ is given by:

$$s_k(t)=\sqrt{Es}\cdot x_{u_{k-L+1}^k}(t)\cdot e^{j\phi_k} \tag{5}$$

The transmitted signal undergoes a phase rotation θ and is corrupted by an additive complex white Gaussian noise (AWGN), $n(t)$, with noise spectral density N_0. θ is assumed to be unknown and uniformly distributed on $[0,2\pi[$. The channel is said to be non-coherent. The corresponding complex-baseband received signal is given by $\forall\, t\in[kT;(k+1)T)$,

$$r_k(t)=e^{j\theta}\cdot s_k(t)+n(t), \tag{6}$$

In this paper, perfect frequency and time synchronization is assumed. During the k^{th} symbol interval, the received signal $r_k(t)$ is passed through a bank of M^L matched filters whose impulse responses are given by $\bar{x}_i(-t)$, $i=0,...,M^L-1$ where $\bar{x}_i(t)$ is the complex conjugate of $x_i(t)$. The sufficient statistics are the samples $r_{i,k}$ resulting from the correlation between $r_k(t)$ and $\bar{x}_i(-t)$.

$$r_{i,k}=\int_0^T r_k(t)\bar{x}_i(t)dt \tag{7}$$

In the sequel, we adopt the following notation $\boldsymbol{r}_k=[r_{0,k},...,r_{M^L-1,k}]$ and the set of observations is given by $\boldsymbol{r}_0^{N_s-1}=[\boldsymbol{r}_0,...,\boldsymbol{r}_{N_s-1}]$.

A trellis-based symbol MAP detection is performed by the BCJR algorithm [14]. This latter computes the conditional probability of a symbol given the observations noted $p(u_k|\boldsymbol{r}_0^{N_s-1})$. Let $\delta_k=\{\phi_{k-N+1},u_{k-N-L+2},...,u_{k-1}\}$ be a state of the trellis. It takes into account the accumulated phase and a series of $N+L-2$ symbols $u_{k-N-L+2}^{k-1}$ at the k^{th} symbol interval (with $k\geq N+L-2$). We can differentiate the $L-1$ symbols coming from the memory required by the partial response (if full-response CPMs are considered, $L=1$ and this amount is null) and the $N-1$ additional symbols required when we extend the observation length in non-coherent regime to improve the performance (if the observation length is one, this amount is null). The transition $\{\delta_k\to\delta_{k+1}\}$ corresponds to the emitted symbol u_k. Following [10], the conditional probability is written as follows

$$\begin{aligned}p(u_k|\boldsymbol{r}_0^{N_s-1})\propto&\sum_{\{\delta_k\}}\alpha_k(\delta_k)\beta_{k+1}(\delta_{k+1})\\&\cdot\gamma(\delta_k\to\delta_{k+1},\boldsymbol{r}_{k-N+1}^k)p(u_k)\end{aligned} \tag{8}$$

The branch metric associated to the non-coherent TBR requires the computation of the conditional probability related to γ and given for any CPM by ([4])

$$\gamma(\delta_k\to\delta_{k+1},\boldsymbol{r}_{k-N+1}^k)\propto I_0\left(\rho\cdot\left|\mu(u_{k-N-L+2}^k)\right|\right) \tag{9}$$

where $\rho{=}2\sqrt{Es}/N_0$ and,

$$\mu(u_{k-N-L+2}^{k}){=}\sum_{i=k-N+1}^{k} r_{u_{i-L+1}^{i},i}\cdot e^{-j2\pi h\sum_{n=k-N-L+2}^{i-L} u_n}$$

The forward-backward recursions read as follows

$$\begin{aligned}\alpha_k(\delta_k) &\propto\sum_{\{\delta_{k-1}\}}\alpha_{k-1}(\delta_{k-1})\frac{I_0\left(\rho\left|\mu(u_{k-N-L+1}^{k-1})\right|\right)}{I_0\left(\rho\left|\mu(u_{k-N-L+2}^{k-1})\right|\right)}p(u_{k-1})\\ \beta_k(\delta_k) &\propto\sum_{\{\delta_{k+1}\}}\beta_{k+1}(\delta_{k+1})\frac{I_0\left(\rho\left|\mu(u_{k-N-L+2}^{k})\right|\right)}{I_0\left(\rho\left|\mu(u_{k-N-L+2}^{k-1})\right|\right)}p(u_{k})\end{aligned} \tag{10}$$

Based on these equations, soft iterative detection and decoding can be performed.

III. Non-coherent Precoding

A. Precoding procedure

Henceforth we denote $\bar{\delta}_k{=}\{\bar{\phi}_{k-N+1}, \bar{u}_{k-N-L+2}, ..., \bar{u}_{k-1}\}$ the precoded TBR state where $\bar{\phi}_{k-N+2}{=}\bar{\phi}_{k-N+1} + 2\pi h\cdot \bar{u}_{k-N-L+2}$. Precoded symbols are computed as follows:

$$\bar{u}_k{=}u_k \oplus a_k \tag{11}$$

Here $\oplus$ is the sum over $\mathbb{Z}_2^m$, so the m bits of u_k are added modulo 2 to the m bits of a_k.

$$\boldsymbol{a}_k{=}\left[\bar{\boldsymbol{u}}_{k-1}, ..., \bar{\boldsymbol{u}}_{k-L+1}, \boldsymbol{\sigma}(\bar{u}_{k-N-L+2}^{k-L})\right]\times\mathbf{F}^{\top} \tag{12}$$

where $\times$ is the matrix product and

$$\sigma(\bar{u}_{k-N-L+2}^{k-L}){=}\sum_{i=k-N-L+2}^{k-L}{}_{Q}\ \bar{u}_i$$

$\bar{\boldsymbol{u}}_i$ is the *right-to-left* binary representation of symbol $\bar{u}_i$ such as $\bar{\boldsymbol{u}}_i{=}[\bar{u}_{0,i}, ..., \bar{u}_{j,i}, ..., \bar{u}_{m-1,i}]$ with $\bar{u}_{j,i}$ the j^{th} bit of $\bar{u}_i$ (the same applies for $\boldsymbol{a}_k$ with a_k). As well $\boldsymbol{\sigma(.)}$ is the *right-to-left* binary representation of $\sigma(.)$ and $\sum_Q$ is the sum $modulo\ Q$. $\mathbf{F}^{\top}$ is the transpose of the $m\times r$-dimensional matrix $\mathbf{F}$ which components belong to $\mathbb{Z}_2$ with $r{=}m\cdot(L-1)+\lceil log_2(Q)\rceil$, where $\lceil\cdot\rceil$ rounds to the next larger integer. For the ease of presentation, an example of a precoding scheme inside the CPE structure is given 1 for a quaternary CPM with $Q{=}4$, $L{=}2$, $\mathbf{F}{=}[1\,3\,1\,3]$ and an observation length of 3 symbols (i.e $N{=}3$). Henceforth, for ease of reading, decimal representation of $\mathbf{F}$ will be considered i.e $\mathbf{F}{=}[1\,3\,1\,3]_{base\,10}$ instead of $\mathbf{F}{=}\begin{bmatrix}1&1&1&1\\0&1&0&1\end{bmatrix}_{base\,2}$. The difference between the dynamic mapping proposed in [6] and the proposed precoding scheme dwells in the accumulated phase: since the coherent time is limited to the observation length in non-coherent regime, only the accumulated symbols from the start of the observation will be taken into account in the precoding scheme.

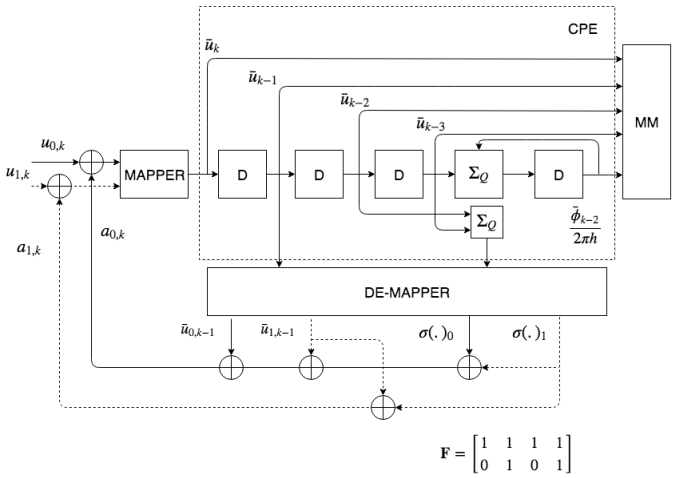

Fig. 1. CPE diagram quaternary CPM with $\mathbf{F}{=}[1\,3\,1\,3]$, $L{=}2$ and $N{=}3$

B. Optimization procedure

EXIT chart helps to visually characterize the exchange of extrinsic information between two or several soft input-soft output (SISO) concatenated components. It is used to analyze the convergence behaviour during the iterative decoding process of BICM scheme. In the coherent case, it can be shown that, if no specific precoding is used most of CPM in use have EXIT transfer function reaching the point $(1,1)$. This enables the use of serially concatenated convolutional outer codes to design simple BICM CPM schemes with no asymptotic error floors: there exists a threshold in terms of E_s/N_0 above which we can achieve an arbitrary low probability of error. The same thing can be achieved with sparse graph codes [16]. However, this is no longer the case in the non-coherent regime where EXIT curves do not reach the point $(1,1)$ as it can be seen in Fig.2 and 3. For an outer convolutional code, it will lead to an asymptotic error floor due to a crossing point between the outer convolutional code and the inner SISO CPM detector, since the decoding process cannot be enhanced: the probability of error is decreasing with an increasing E_s/N_0 but it is bounded away from zero. We aim at designing a precoding scheme ensuring efficient iterative decoding (no asymptotic error floor) while enabling the same performance of the coherent regime. Matrices $\mathbf{F}$ are obtained by a brute-force method meaning that the 2^{rm} possible precoding schemes are tested and we select those converging to point $(1,1)$. The set of matrix enabling the convergence to point $(1,1)$ is noted $\mathcal{F}_c$. It has been observed that, based on the proposed precoding procedure, various EXIT trajectories with equal information rate can be obtained for a given modulation and operating point. So, additionally, we select the EXIT curves with the highest extrinsic information corresponding to zero apriori information. Consequently the optimize $\mathbf{F}$ matrix must be included in $\mathcal{F}_c$ and should have the highest extrinsic information for zero apriori among this set. The latter condition offers the best pragmatic capacity among $\mathcal{F}_c$, ie. if no iterative decoding is used. Various CPM optimal matrix $\mathbf{F}$ are displayed in Table I.

TABLE I
CPM OPTIMAL MATRIX FOR NON-COHERENT PRECODING

CPM	**F**	h	M	L
[8] Weighted (AV) (α_{rc}=0.75)	[1 1 0 0]	1/3	Quaternary	2
GMSK (BT_s=0.25)	[1 0]	1/2	Binary	2
RC	[1 1 0 0]	1/4	Quaternary	2
CPFSK	[1 1 0]	5/7	Quaternary	1

IV. SIMULATION RESULTS

EXIT charts has been traced with an observation length of 2 symbols (i.e N=2) for: (a) a binary GMSK for an operating point of E_s/N_0=2.5 dB in Fig.2 and (b) a quaternary 2RC for an operating point of E_s/N_0=4.5 dB in Fig. 3. Two cases were considered in the non-coherent regime: a first EXIT curve has been plotted without precoding and a second one was plotted with an optimized matrix **F**=[1 0] (respectively **F**=[1 1 0 0] with the 2RC modulation). This matrix was obtained by the previous optimization procedure. Convolutional code EXIT chart of rate one-half with polynomials (5,7) in octal has been added Fig.2 and 3. It appears that the non-precoding EXIT curve intersects the convolutional code contrary to the one with the optimal precoding. Consequently, without precoding, the iterative procedure between the outer convolutional code and the CPM demodulator is stopped at the crossing level. This interruption in the decoding process will trigger an error floor (see Fig. 4 and 5). Furthermore non-coherent precoded and unprecoded EXIT curves in coherent regime were also studied. It seems that the non-coherent precoding has no effect to the coherent TBR probably due to the fact that it does not include the accumulated phase. Then the bit error rates (BER) for the GMSK and 2RC modulation have been traced on Fig. 4 and 5 for the non-coherent regime (noted N.C. on the graph). Binary messages were encoded by the considered rate one-half convolutional encoder for several coding length (N_b=512, 2048, and 16000 bits). The unprecoded case is also reported. As expected, performance are enhanced by the precoded scheme, underlying the relevant use of CPM precoding in non-coherent regime. We can clearly observe that the BER of the precoding systems are characterized by the so called *waterfall* transition whereas an error floor impairs the unprecoded systems performance. In addition, we can also notice that the coding length has an impact on the system performance. A large coding length behaves better than smaller one.

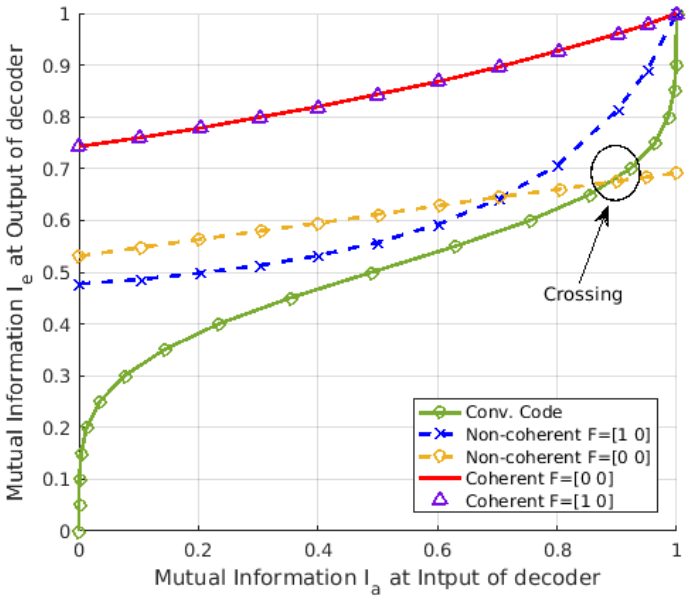

Fig. 2. Exit charts binary GMSK with h=$\frac{1}{2}$, L=2 and BT=0.25.

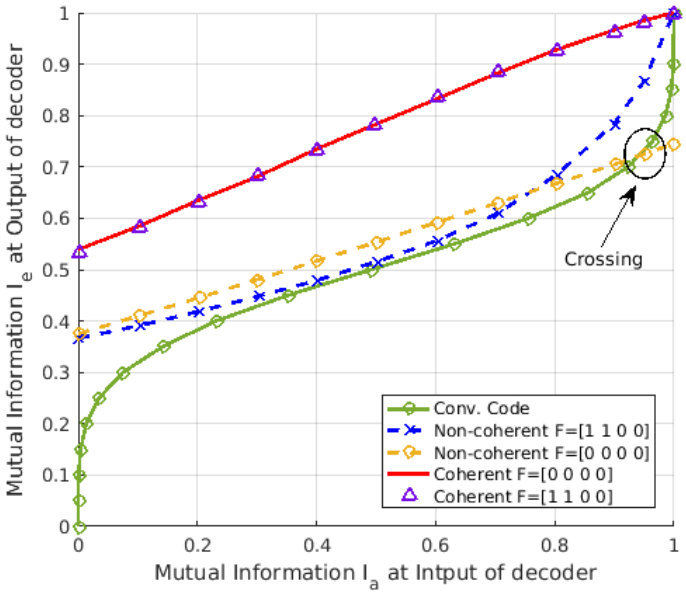

Fig. 3. Exit charts quaternary 2RC with h=$\frac{1}{4}$ (naural mapping).

V. CONCLUSION

Classical mapping between information symbols and CPM waveforms in the non-coherent regime yields EXIT charts which do not converge to point $(1, 1)$ as in the coherent case. Therefore CPM modulation serially concatenated with a classical convolutional code generates error floors in the non-coherent regime. To deal with this issue, a precoding has been added in the CPM trellis structure. The precoding impacts EXIT trajectories making them, in somes cases, convergent

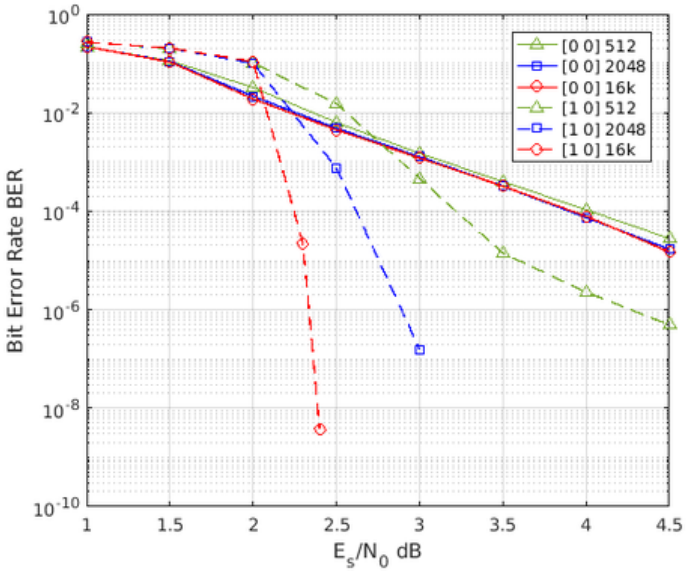

Fig. 4. BER N.C. binary GMSK with $h{=}\frac{1}{2}$, $L{=}2$ and $BT{=}0.25$.

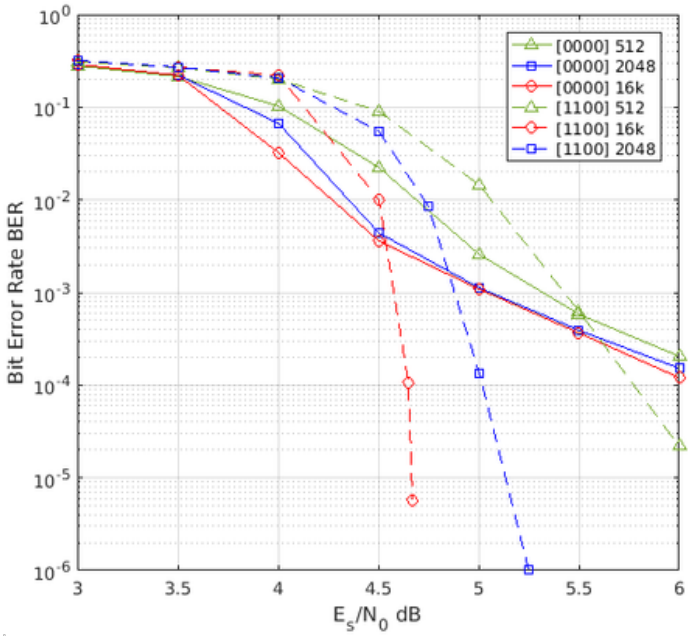

Fig. 5. BER N.C. quaternary 2RC with $h{=}\frac{1}{4}$ (natural mapping)

to point $(1,1)$. As a result, when the precoding is optimally chosen among the ones yielding EXIT curves converging to point $(1,1)$, the error floor is removed. This demonstrates the relevant use of CPM precoding in non-coherent regime. Moreover, the proposed precoding does not influence the behavior of the coherent SISO CPM receiver enabling efficient operation in both regimes. In the near future, combination of precoding with sparse graph based code optimization will be investigated.

REFERENCES

[1] J. G. Proakis, "Characterization of Communication Signals and Systems" in "Digital Communication", 4^{th} ed. New York: Irwin/McGraw-Hill, 2001, ch.4, sec.3, pp.185-189.

[2] J. B. Anderson, T. Aulin and C.-E. Sundberg "Digital Phase Modulation" Springer Science & Business Media, 2013.

[3] B. E. Rimoldi, "A Decomposition Approach to CPM", *IEEE Trans. on information theory*, vol. 34, no. 2, pp 260-270 March. 1988.

[4] M. C. Valenti, S. Cheng and D. Torrieri, "Iterative Multisymbol Noncoherent Reception of Coded CPFSK", *IEEE Transaction on communications*, vol. 58 no. 7, pp 2046-2054 July. 2010.

[5] Shi Cheng, Mattew C. Valenti and Don Torrieri, "Coherent Continuous-Phase Frequency-Shift Keying: Parameter Optimization and Code Design", *IEEE Transaction on wireless communications*, vol. 8 no. 4, pp 284-287, April. 2009.

[6] S. Benedetto, G. Montorsi, A. Perotti and A. Tarable, "A Pragmatic Approach to Coded Continuous-Phase Modulation," 2007 Information Theory and Applications Workshop, La Jolla, CA, 2007, pp. 36-40

[7] A. Perotti, A. Tarable, S. Benedetto and G. Montorsi, "Capacity-Achieving CPM Schemes," in IEEE Transactions on Information Theory, vol. 56, no. 4, pp. 1521-1541, April 2010.

[8] ETSI EN 301 545-2 V1.1.1. Digital video broadcasting (dvb); second generation dvb interactive satellite system (dvb-rcs2); part 2: Lower layers for satellite standard. 2013.

[9] C.-U. Piat-Durozoi, C. Poulliat, M.-L. Boucheret, N. Thomas and G. Lesthievent "On sparse graph coding for coherent and noncoherent demodulation," IEEE ISIT, Aachen, June 2017.

[10] C.-U. Piat-Durozoi, C. Poulliat, M.-L. Boucheret, N. Thomas, E. Bouisson and G. Lesthievent "Multisymbol with memory noncoherent detection of CPFSK," IEEE ICASSP, New-Orleans, March 2017.

[11] T. Benaddi, "Sparse graph-based coding schemes for continuous phase modulations", PhD Thesis, INP Toulouse, Dec. 2015.

[12] T. Benaddi, C. Poulliat, M.-L. Boucheret, B. Gadat, G. Lesthievent, "Design of Unstructured and Protograph-Based LDPC Coded Continuous Phase Modulation," in proc. IEEE ISIT, Honolulu, HI, USA, 2014.

[13] G. Colavolpe, G. Ferrari and R. Raheli, "Noncoherent Iterative (Turbo) Decoding", *IEEE Transaction on communications*, vol. 48 no. 9, pp 1488-1498 September. 2000.

[14] L. Bahl, J. Cocke, F. Jelinek and J. Raviv, "Optimal Decoding of Linear Codes for Minimizing Symbol Error Rate", *IEEE Transaction on Information Theory*, vol IT-20, pp 284–287, March 1974.

[15] S. Ten Brink, "Convergence Behaviour of Iteratively Decoded Parallel Concatenated Codes", *IEEE Transaction on communications*, vol. 49 no. 10, pp. 1727-1737, October. 2001.

[16] S. ten Brink, G. Kramer, and A. Ashikhmin, "Design of low-density parity-check codes for modulation and detection," *IEEE Transaction on communications* vol. 52, no. 4, pp. 670-678, April 2004.

[17] J. Hagenauer "The EXIT chart-introduction to extrinsic information transfer in iterative processing", Proc. 12th European Signal Processing Conference (EUSIPCO). pp. 1541–1548 2004.